Published in final edited form as:
Mol Cancer Ther. 2008 September ; 7(9): 2828–2836. doi:10.1158/1535-7163.MCT-08-0336.

17α-Hydroxylase/17,20 lyase inhibitor VN/124-1 inhibits growth of androgen-independent prostate cancer cells via induction of the endoplasmic reticulum stress response

Robert D. Bruno[1], **Tony D. Gover**[1], **Angelika M. Burger**[1,2], **Angela M. Brodie**[1,2], and **Vincent C. O. Njar**[1,2]

[1]Department of Pharmacology and Experimental Therapeutics, University of Maryland School of Medicine, Baltimore, Maryland [2]University of Maryland Marlene and Stewart Greenebaum Cancer Center, School of Medicine, Baltimore, Maryland

Abstract

Inhibitors of the enzyme 17α-hydroxylase/17,20 lyase are a new class of anti–prostate cancer agents currently undergoing preclinical and clinical development. We have previously reported the superior anticancer activity of our novel 17α-hydroxylase/17,20 lyase inhibitor, VN/124-1, against androgen-dependent cancer models. Here, we examined the effect of VN/124-1 on the growth of the androgen-independent cell lines PC-3 and DU-145 and found that the compound inhibits their growth in a dose-dependent manner *in vitro* (GI_{50}, 7.82 μmol/L and 7.55 μmol/L, respectively). We explored the mechanism of action of VN/124-1 in PC-3 cells through microarray analysis and found that VN/124-1 up-regulated genes involved in stress response and protein metabolism, as well as down-regulated genes involved in cell cycle progression. Follow-up real-time PCR and Western blot analyses revealed that VN/124-1 induces the endoplasmic reticulum stress response resulting in down-regulation of cyclin D1 protein expression and cyclin E2 mRNA. Cell cycle analysis confirmed G_1-G_0 phase arrest. Measurements of intracellular calcium levels ($[Ca^{2+}]_i$) showed that 20 μmol/L VN/124-1 caused a release of Ca^{2+} from endoplasmic reticulum stores resulting in a sustained increase in $[Ca^{2+}]_i$. Finally, cotreatment of PC-3 cells with 5, 10, and 20 μmol/L VN/124-1 with 10 nmol/L thapsigargin revealed a synergistic relationship between the compounds in inhibiting PC-3 cell growth. Taken together, these findings show VN/124-1 is endowed with multiple anticancer properties that may contribute to its utility as a prostate cancer therapeutic.

Introduction

Prostate cancer is the most common malignancy and second leading cause of cancer-related deaths in men in the western world. The American Cancer Society estimates that, in 2008,

Requests for reprints: Vincent C.O. Njar, University of Maryland Baltimore, School of Medicine, 685 West Baltimore Street, HSF Room 580 I, Baltimore, MD 21201-1559. Phone: 410-706-5882; Fax: 410-706-0032. vnjar001@umaryland.edu.

Disclosure of Potential Conflicts of Interest
No potential conflicts of interest were disclosed.

186,320 new cases will be diagnosed and 28,660 patients will die from the disease in the United States alone (1). Despite advances in screening and treatment of localized disease, advanced prostate cancer remains incurable.

Androgens play a vital role in the development, growth, and progression of prostate cancer (2). Therefore, androgen deprivation therapy remains the standard treatment for advanced prostate cancer. Current androgen deprivation therapy includes treatment with luteinizing hormone releasing hormone agonists and/or androgen receptor (AR) antagonists. Unfortunately, luteinizing hormone releasing hormone agonists fail to inhibit release of adrenal androgens and AR antagonists have been shown to act as partial agonists in prostate cancer cells expressing mutated and/or overexpressed AR (3, 4).

An alternative strategy for androgen deprivation therapy is the global inhibition of androgen synthesis. This can be accomplished through the inhibition of the enzyme 17α-hydroxlase/17,20-lyase (CYP17), which catalyzes two sequential and necessary reactions in the production of androgens (5). The imidazole antifungal agent ketoconazole, a nonspecific cytochrome P450 inhibitor, has been used for this indication and has shown modest efficacy in patients no longer responding to antiandrogen treatment (6, 7).

Ketoconazole treatment is, unfortunately, limited by toxicity due to its lack of specificity for CYP17. However, specific CYP17 inhibitors are emerging as a promising new class of anti–prostate cancer agents. One such molecule, abiraterone (17-(3-pyridyl)androsta-5,16-dien-3β-ol), has entered phase II clinical trials, wherein it has shown efficacy in castration refractory prostate cancer patients (8, 9). Our laboratory has carried out extensive research in this field and developed several molecules that inhibit both CYP17 and the AR directly (10). One of these compounds, a 17-benzoimidazole called VN/124-1 (Fig. 1A), has demonstrated excellent anticancer properties both *in vitro* and *in vivo* and has been shown to inhibit the growth of LAPC4 tumor xenografts more effectively than castration (11). Superior efficacy of VN/124-1 over castration in mice—which, unlike humans, do not express CYP17 in their adrenal glands and, therefore, do not secrete adrenal androgens (12)—lead us to hypothesize that the compound may have activity against androgen-independent prostate cancer cells as well. We now report that VN/124-1 and structurally related CYP17 inhibitors, including abiraterone, inhibit the growth of the androgen-independent cell lines PC-3 and DU-145 and identify the endoplasmic reticulum stress response (ERSR) as the mechanism of growth inhibition of the compound. Importantly, these effects were seen at concentrations previously shown to be achievable in both plasma and within tumors in mouse prostate cancer xenograft models (11).

As the center of protein-folding, the endoplasmic reticulum (ER) is extremely sensitive to disruptions in homeostasis, including disruptions in calcium concentrations. Such stresses induce the ERSR, also called the unfolded protein response. The ERSR is an evolutionarily conserved pathway that seeks to relieve the build-up of unfolded proteins in the ER. To achieve this, the cell first up-regulates ER resident molecular chaperones, such as glucose-regulated protein 78 (gp78/BiP; refs. 13–15), and reduces ER load through phosphorylation of the α subunit of the eukaryotic translation initiation factor 2α (eIF2α; refs. 16, 17). Phosphorylation of eIF2α results in attenuation of translation of nonessential proteins,

including growth-related proteins, such as cyclin D1 (18–22). Although the ERSR is a survival pathway, prolonged stimulation of the ERSR results in growth arrest and apoptosis via the up-regulation of apoptotic-related proteins, including the CCAAT/enhancer-binding protein homologous transcription factor (CHOP; ref. 23). As a result, ERSR has been implicated in the anticancer activities of many synthetic and natural cancer therapeutics, including clotrimazole, fatty acid synthase inhibitors, Cox-2 inhibitors, $3^1 3^1$-diindolylmethane, and eicosapentaenoic acid (19, 24–27).

We show that VN/124-1 induces ERSR, resulting in the up-regulation of ERSR-associated genes and the phosphorylation of eIF2α. This leads to the inhibition of cyclin D1 translation, resulting in G_1 arrest. Analysis of intracellular calcium signaling reveals that VN/124-1 causes the release of Ca^{2+} from ER, resulting in the depletion of ER calcium stores, and a sustained increase in intracellular Ca^{2+} concentrations ($[Ca^{2+}]_i$).

As VN/124-1 has recently been licensed to Tokai Pharmaceuticals, Inc. for clinical development, a complete understanding of the mechanism of actions of the molecule is important. These findings underscore the potential of VN/124-1 as an effective therapeutic for androgen-dependent and androgen-independent prostate cancer.

Materials and Methods

Compounds

VN/63-1, VN/85-1, VN/124-1, VN/125-1, and abiraterone were synthesized in our laboratory, as previously described (11, 28–30). Thapsigargin, cyclopiazonic acid, and dihydroandrosterone (DHA) were purchased from Sigma Aldrich. Compounds were dissolved in either 95% ethanol or DMSO. For all experiments, control cells were dosed with equal volume of vehicle (0.1% or less), as used in the treated groups.

Cell Culture and Viability Assays

All cell lines were obtained from American Type Culture Collection and maintained in RPMI 1640 supplemented with 10% fetal bovine serum and 5% penicillin/streptomycin solution. Cells were grown as a monolayer in a humidified incubator (5% CO_2) at 37°C. To determine the effect of compounds on cell proliferation, cells were plated (2,500 cells per well) in 96-well cell culture dishes (Corning, Inc.). After a 24-h attachment period, medium was replaced with fresh medium containing compounds (0.01–100 μmol/L) or vehicle (95% ethanol). The cells were then allowed to grow in the presence of the drugs for 96 h. After 96 h, relative cell viability was assessed using the MTT reagent [3-(4,5-dimethylthiazol-2-yl)-2,5-diphenyltetrazolium bromide], as described in Patel et al. (31). Experiments were carried out thrice with six replicates per dose per experiment ($n = 18$). Results were plotted using the average of each dose over all three experiments and fitted with a best-fit sigmoidal dose response variable slope curve using GraphPad Prism 4.01 (GraphPad Software, Inc.). For combination of VN/124-1 and thapsigargin, cells were treated for 72 h and viability was assessed as described for single agents. Combination index was calculated, as previously described (32). Combination index values of <1 are considered synergistic.

Microarray

PC-3 cells were treated with (95% ethanol) or 20 μmol/L of VN/124-1. After 24-h exposure to the agent, total RNA was isolated using the Qiagen RNeasy-Mini kit following manufacturer's protocol. Experiments were carried out in duplicate, with triplicate samples (dosed independently on three different days) from each experiment pooled for analysis on a single chip. Samples were hybridized to a GeneChip Human Genome Focus Array (Affymetrix, Inc.) and analyzed using an Affymetrix Genechip Scanner 3000 according to manufacturer's protocol. Gene ontologies were identified using the online Database for Annotation, Visualization, and Integrated Discovery provided by National Institute of Allergy and Infectious Diseases and NIH. Only genes that were up-regulated or down-regulated by an average of ≥2-fold and had a minimum 1.5-fold change (up or down) per array were used for this analysis. Genes that showed ≥1.5-fold change (up or down) in control samples on one or both chips were excluded. Stringent criteria of a minimum EASE/*P* value threshold of 0.001 and a gene count threshold of 5 were used to identify altered gene ontologies.

Real-Time PCR

Cells were treated and lysed, and RNA were collected and quantified using the same method outlined above. Cells were dosed independently on three separate days ($n = 3$). One microgram of total RNA was converted to cDNA using ReactionReady First Strand cDNA Synthesis kit (SuperArray Bioscience Corp.) following the manufacturer's protocol. Template cDNA (50 ng) was then used in subsequent quantitative real-time PCR (qRT-PCR) reactions. Template was combined with target gene specific or β-actin control RT^2 PCR Primer Sets, RT^2 Real-Time™ SYBR Green/Rox Master Mix (SuperArray Bioscience Corp.), and double-distilled water for a final reaction volume of 25 μL and run on a 7900HT Fast Real-Time PCR system (Applied Biosystems) following the manufacturer's protocol. Fold changes were calculated using the $\Delta\Delta C_t$ method, as recommended by the manufacture's protocol.

Cell CycleAnalysis

Cells were synchronized in the G_1-G_0 phase by maintaining them in 0.2% fetal bovine serum–containing medium for 96 h. After starvation, medium was replaced with normal growth medium (10% fetal bovine serum) containing vehicle (95% ethanol) or 20 μmol/L VN/124-1 for 12, 18, and 24 h. At each time point, cells were fixed in 70% ethanol at −20°C for at least 24 h. Fixed cells were then incubated with 1 mL propidium iodide staining buffer (1 mg/mL propidium iodide, 0.1% Triton-X, and 10 μg/mL RNase A dissolved in PBS) for 1 h at room temperature, and DNA content was measured by flow cytometry analysis using a FACSort flow cytometer (Becton Dickinson); 15,000 events were analyzed for each sample. ModFit LT version 3.1 (Verity Software House Ind.) was used to analyze cell cycle distribution.

Western Blot

Cells were treated with VN/124-1, DHA, thapsigargin, or vehicle for 6 and 24 h. Protein was isolated, subjected to SDS-PAGE, transferred, and imaged, as previously described (33). All

primary antibodies were purchased from Cell Signaling. Quantitation of relative protein expression was determined via densitometry using the software ImageQuant 5.0 (Molecular Dynamics), with each protein normalized to its respective loading control. Results represent the average of at least three independent experiments, with representative blots shown.

Ca^{2+} Measurements

PC-3 Cells were loaded with either fura-2 or fluo-3 indicator by incubation with 2 μmol/L fura-2/AM or 2 μmol/L fluo-3/AM in RPMI 1640 containing 10% fetal bovine serum for >60 min at room temperature. During experiments, the coverslips were mounted in a flow chamber and superfused with oxygenated Locke solution containing (in mmol/L) 10 glucose, 136 NaCl, 5.6 KCl, 1.2 NaH_2PO_4, 14.3 $NaHCO_3$, 1.2 $MgCl_2$, and 2.2 $CaCl_2$ (pH 7.4) at room temperature (22–24°C).

For measurement of $[Ca^{2+}]$ in individual cells, PC-3 cells were treated with 1, 5, 10, and 20 μmol/L VN/124-1, 20 μmol/L DHA, or vehicle. Cells loaded with fura-2 were placed in a perfusion chamber mounted on an inverted microscope (TE200; Nikon) equipped with a UV-transmitting objective (SuperFluor, 40×, N.A. 1.4, Nikon). Fura-2 was alternately excited by 340 and 380 nm light from monochrometers (Deltascan Illumination System, Photonic Technology International), and fura-2 emission was passed through a 515-nm longpass filter before detection by a cooled CCD camera (Retiga 2000R, Q-Imaging). For measurement of Ca^{2+} transients in individual cells, cover-slips with fluo-3 loaded cells were excited by the output of a 100-W mercury arc lamp that passed through a 480-nm bandpass filter (30 nm bandwidth). Fluorescence emission was passed through a 515-nm longpass filter before capture by a cooled CCD camera (Retiga 2000R, Q-Imaging). Image acquisition was done with QCapture Pro (Q-Imaging), and analysis was done with ImageJ (U.S. NIH).

Fluo-3 Ca^{2+} indicator measurements are reported as the fractional change in fluorescence intensity relative to baseline ($\Delta F/F_0$), which was determined as follows. Within a temporal sequence of fluorescence images, a region of interest was drawn around each cell to be analyzed. The fluorescence signal from each cell was calculated as the pixel-averaged intensity within each region of interest. In these experiments, we typically observed a slight downward drift in baseline, which was principally attributable to photo-bleaching of the indicator. In such cases, the drift was always well fit by a low-amplitude single-exponential decay. The fitted baseline value (F_0) at every time point was then used to calculate $\Delta F/F_0$. $\Delta F/F_0$ values are reported as mean ± SE. For fura-2 measurements, $[Ca^{2+}]_i$ was derived using the ratio method of Grynkewicz et al. (34).

Statistical Analysis

qRT-PCR results for each gene were analyzed via a Student's *t* test comparing ΔC_t values (C_t value of test gene minus β-actin control). Western blots and combination growth studies were analyzed with Kruskal-Wallis and Dunn's multiple comparison post-hoc tests. Flow cytometry data was analyzed with Student's *t* test. $[Ca^{2+}]_i$ data was analyzed with one-way ANOVA with Dunnett's post-hoc test.

Results

VN/124-1 and Related C-17 Steroidal Azolyl Compounds Inhibit the Growth of Androgen-Independent Prostate Cancer Cell Lines

To determine if VN/124-1 exerts a direct cytotoxic/cytostatic effect, we treated the androgen-independent prostate cancer cell lines PC-3 and DU-145 with increasing concentrations of VN/124-1 and found that the compound inhibited both cell lines in the low micromolar range (Fig. 1B–D; Table 1). The potency of VN/124-1 against PC-3 and DU-145 cell lines was comparable with that seen with androgen-dependent LNCaP cells (low micromolar range). Structurally related steroidal C-17–substituted lyase inhibitors VN/63-1, VN/85-1, VN/125-1, and abiraterone also inhibited the growth of PC-3 and DU-145 cells (Table 1). The structurally related androgen DHA, however, was almost a 10-fold less potent than VN/124-1 in inhibiting PC-3 cells and lacked any growth inhibitory activity against DU-145 cells up to 100 μmol/L. Inhibition of LNCaP cell viability *in vitro* was previously attributed to the ability of VN/124-1 to act as an AR antagonist. However, as PC-3 and DU-145 cells are well-established androgen-independent cell lines that do not express a functional AR (35), it is clear from these results that these compounds also have activities distinct from the androgen axis.

Microarray Analysis Reveals VN/124-1 Induces the Down-regulation of Cell Cycle – Related Genes and Up-regulation of Genes Involved in Cellular Response to Stress in PC-3 Cells

To shed light on the mechanism of action of VN/124-1, PC-3 cells were treated with 20 μmol/L (~GI_{90}) of the compound for 24 hours and global gene expression changes were measured using a GeneChip Human Genome Focus Array. We used the online Database for Annotation, Visualization, and Integrated Discovery to identify clusters of related genes affected by VN/124-1. As shown in Table 2 (*top*), the most enriched up-regulated ontologies are those relating to stress and metabolism, in particular amino acid metabolism. Nearly all of the down-regulated ontologies (Table 2, *bottom*) are associated with the cell cycle, especially the S-phase (DNA replication). Interestingly, induction of genes involved in amino acid metabolism has been shown to occur after induction of ER stress (36), and the ERSR is known to block the transition to S-phase of the cell cycle. These preliminary findings lead us to hypothesize that VN/124-1 may inhibit growth via induction of the ERSR.

VN/124-1 Induces Genes Involved in ER-Stress Response

We next sought to validate the gene expression changes of specific genes found to be altered by VN/124-1 in the microarray experiment by using qRT-PCR (Fig. 2A). The most highly up-regulated gene found in the microarray was S100P calcium binding protein (S100P). S100P is a member of the S100 family of proteins, all of which take part in Ca^{2+} signaling. Surprisingly, S100P has been shown to be involved in the growth and survival of cancer cells and is a negative prognostic marker of disease progression (37, 38). The functional significance of this remains unknown, but interestingly, S100P has been reported to be up-regulated by other chemotherapeutics and natural anticancer agents, including DNA cross-linking agents and all-*trans* retinoic acid (39, 40). Other genes verified by qRT-PCR that were up-regulated in the microarray experiment include asparagines synthetase and

activating transcription factor 4. Both of these genes have been reported to be up-regulated by the ERSR (25). CHOP was not included in the microarray but is a marker for the ERSR (23), and qRT-PCR revealed it to be strongly up-regulated by VN/124-1. We also looked at the expression of the G_1 cyclins D1 and E2. Interestingly, cyclin D1 mRNA levels were not affected by VN/124-1, but the downstream cyclin E2 was significantly reduced. These results were very similar to those seen in the microarray.

VN/124-1 Induces ERSR-Related Proteins, Phosphorylation of eIF2α, and Down-regulation of Cyclin D1

To confirm ERSR as a mechanism of VN/124-1 action, we next analyzed the effect of the drug at the protein level. PC-3 cells were treated with VN/124-1 for 6 and 24 hours. As shown in Fig. 2B, 20 μmol/L VN/124-1 induced the phosphorylation of eIF2α at 6 and 24 hours. The drug also significantly induced the expression of the molecular chaperone gp78/BiP, a well-established marker of ER stress (13–15), in a dose-dependent manner. As mentioned previously, phosphorylation of eIF2α attenuates translation of many transcripts, including cyclin D1. This was confirmed as VN/124-1 induced the down-regulation of cyclin D1 protein significantly after 24 hours. As discussed above, VN/124-1 had no effect on cyclin D1 mRNA levels, suggesting this down-regulation is indeed occurring at the translational level. Of note, treatment with 20 μmol/L DHA had no significant effect on any of the protein markers measured. Taken together, these findings strongly support the hypothesis that VN/124-1 induces the ERSR.

VN/124-1 Induces G_1-G_0 Growth Arrest

We next analyzed the effect of VN/124-1 on cell cycle distribution in PC-3 cells. We found that treatment with 20 μmol/L VN/124-1 prevented the exit from G_1 phase of the cell cycle in synchronized cells (Fig. 2C). This resulted in a significant increase in the amount of cells in G_1-G_0 at 18 and 24 hours. These findings are in line with the loss of cyclin D1 protein expression and subsequently cyclin E2 transcription, as both are needed for transition to the S-phase of the cell cycle (41). This is also in accord with the microarray data showing VN/124-1 down-regulates genes involved in DNA replication.

VN/124-1 Induces Release of Ca^{2+} from ER Stores

We next sought to answer the question of how VN/124-1 induces ER stress. Some structurally related compounds, including $3^1 3^1$-diindolylmethane and imidazole containing antifungals, such as clotrimazole and eiconazole, have been shown to elicit the ERSR by disrupting ER calcium homeostasis (19, 42, 43). To determine if VN/124-1 induces the ERSR in a similar manner, we treated PC-3 cells with 20 μmol/L VN/124-1 and measured relative changes in intracellular calcium concentrations $[Ca^{2+}]_i$ using the calcium-sensitive fluorescent dye Fluo-3AM. As seen in Fig. 3A, VN/124-1 induced an immediate transient increase in $[Ca^{2+}]_i$ (mean $\Delta F/F_0 = 0.613$). This transient was not reduced when extracellular calcium was removed from the bath (mean $\Delta F/F_0 = 0.967$; Fig. 3B) but was completely abolished when ER calcium stores were depleted by pretreatment with the sarco/ER Ca^{2+}-ATPase inhibitor cyclopiazonic acid (Fig. 3C). Finally, we measured the sustained effect of VN/124-1 on absolute $[Ca^{2+}]_i$ using Fura-2AM. PC-3 cells were treated for 2 hours with

vehicle, DHA, or increasing concentrations of VN/124-1 (Fig. 3D). Control cells had an average $[Ca^{2+}]_i$ of 36.49 nmol/L, whereas cells treated with 5, 10, and 20 μmol/L VN/124-1 had a significant increase in $[Ca^{2+}]_i$ (79.13, 96.63, and 79.89 nmol/L, respectively). Treatment with DHA or 1 μmol/L VN/124-1 did not have a significant effect on $[Ca^{2+}]_i$. These results clearly show that VN/124-1 is inducing Ca^{2+} release from ER stores, resulting in a sustained increase in $[Ca^{2+}]_i$.

VN/124-1 Synergizes with Known ERSR Inducer Thapsigargin

To determine if VN/124-1 would act synergistically with a compound known to induce ER stress, we cotreated PC-3 cells with VN/124-1 and the sarco/ER Ca^{2+}-ATPase pump inhibitor thapsigargin. A subtoxic dose of 10 nmol/L thapsigargin was combined with 5, 10, and 20 μmol/L of VN/124-1, and cell viability was measured after 96 hours. As shown in Fig. 4A, thapsigargin and VN/124-1 act synergistically to inhibit the growth of PC-3 cells at all three concentrations (combination index = 0.40, 0.58, and 0.77, respectively), further implicating the ERSR and calcium disruptions as mechanisms of action of VN/124-1.

Discussion

Inhibitors of CYP17 are an exciting new class of potential prostate cancer therapeutics. As these drugs enter clinical trials, complete understanding of their mechanisms of action is important in evaluating their efficacy and safety. In the present study, we show that the CYP17 inhibitor/antiandrogen VN/124-1, as well as other structurally related CYP17 inhibitors, exerts direct growth inhibitory actions against the androgen-independent cell lines PC-3 and DU-145. As these actions were seen in the low micromolar range, it is important to note that peak plasma concentrations of abiraterone (given clinically as the prodrug abiraterone acetate) are below 1 μmol/L (44), suggesting these findings may not be relevant for that compound. However, preclinical kinetics data of VN/124-1 has shown that concentrations above 20 μmol/L are achievable in mouse *in vivo* models (11), indicating that these findings are physiologically relevant.

Using various molecular, pharmacologic, and biochemical techniques, we were able to identify the likely mechanism of VN/124-1 action against androgen-independent prostate cancer cells (Fig. 4B, *right*). VN/124-1 induces the rapid release of Ca^{2+} from ER, resulting in a sustained increase in $[Ca^{2+}]_i$. This disruption in Ca^{2+} homeostasis induces ERSR, resulting in the up-regulation of ERSR-related genes and the phosphorylation of eIF2α. Phosphorylation of eIF2α attenuates the translation of several progrowth genes, including cyclin D1. The loss of cyclin D1 prevents exit from the G_1-phase of the cell cycle, thereby inhibiting the growth of cells.

It remains unclear how VN/124-1 induces release of Ca^{2+} from ER. Interestingly, the compound was shown to act synergistically with thapsigargin, suggesting VN/124-1 works through a separate mechanism. Still, disruptions in Ca^{2+} and induction of ERSR are likely not to be selective for cancer cells *in vitro*. However, there is a growing belief that agents that induce the ERSR may exhibit some specificity for tumors *in vivo*, as it is well documented that tumors are under constant low levels of ER stress (45). This is in large part due to the hypoxic conditions of the tumor microenvironment. Recent studies with the

ERSR-inducing compound, $3^{1}3^{1}$-diindolylmethane, showed that cancer cells were sensitized to the drug when cotreated not only with thapsigargin but also in medium deficient in leucine and supplemented with 2-deoxyglucose and the Hif1α inducer $CoCl_2$ to simulate the hypoxic and nutrient-deficient environment of the tumor (25). Therefore, it is possible that a therapeutic window exists where VN/124-1 could be used to treat androgen-independent prostate cancer without significant toxicity.

It remains unclear as to how VN/124-1 induces Ca^{2+} release from ER. It may be through a direct or indirect mechanism, such as the production of reactive oxygen species—as has been shown with the imidazole containing antifungal econazole (43). Future studies will seek to answer this question, as well as the efficacy of VN/124-1 against androgen-independent *in vivo* models of prostate cancer.

VN/124-1 seems to be endowed with multiple pharmacologic properties that add to its utility as a prostate cancer therapeutic. Figure 4B outlines all of the androgen-dependent and androgen-independent mechanisms of VN/124-1. The major mechanism of VN/124-1 remains inhibition of CYP17, which is achieved in the low nano-molar range. However, previous studies have shown high doses (0.15 mmol/kg bd) were capable of inhibiting tumors significantly better than castration *in vivo* (11), suggesting that the ability of VN/124-1 to induce ERSR may play a role at such doses. The findings outlined in this study represent a major step forward in the understanding of the mechanism of action of VN/124-1 and underscore its potential to be used to treat all phases of prostate cancer.

Acknowledgments

Grant support: NIH grants R21 CA117991-01 and R01CA027440-28 awarded (V.C.O. Njar, A.M. Brodie). T.D. Gover works in the laboratory of Daniel Weinreich, which is funded by NIH grant R01NS022069-20. R.D. Bruno is supported in part by National Institute of Environmental Health Safety training grant T32 ES007263-16A1.

We thank UMB Bipolymer Core Facility for their assistance in the microarray and qRT-PCR experiments, UMB Flow Cytometry Core Facility for their assistance with cell cycle experiments, and Dr. Daniel Weinrich for the use of his laboratory for Ca^{2+} measurement studies.

References

1. ACS. Cancer Facts and Figures 2008. Atlanta: American Cancer Society; 2008.
2. McConnell JD. Physiologic basis of endocrine therapy for prostatic cancer. Urol Clin North Am. 1991; 18:1–13. [PubMed: 1899494]
3. Chen CD, Welsbie DS, Tran C, et al. Molecular determinants of resistance to antiandrogen therapy. Nat Med. 2004; 10:33–9. [PubMed: 14702632]
4. Fuse H, Korenaga S, Sakari M, et al. Non-steroidal antiandrogens act as AF-1 agonists under conditions of high androgen-receptor expression. Prostate. 2007; 67:630–7. [PubMed: 17342748]
5. Hall PF. Cytochrome P-450 C21scc: one enzyme with two actions: hydroxylase and lyase. J Steroid Biochem Mol Biol. 1991; 40:527–32. [PubMed: 1958554]
6. Small EJ, Baron AD, Fippin L, Apodaca D. Ketoconazole retains activity in advanced prostate cancer patients with progression despite flutamide withdrawal. J Urol. 1997; 157:1204–7. [PubMed: 9120902]
7. Trachtenberg J, Halpern N, Pont A. Ketoconazole: a novel and rapid treatment for advanced prostatic cancer. J Urol. 1983; 130:152–3. [PubMed: 6306286]
8. Reid, AHM.; Attard, G.; Molife, R., et al. Abiraterone, an oral, irreversible CYP450c17 enzyme inhibitor appears to have activity in post-docetaxel castration refractory prostate cancer patients.

98th Annual Meeting for American Association for Cancer Research; 2007 April 17; Los Angeles, CA. 2007.

9. Attard, G.; Reid, AHM.; Barrett, M., et al. Inhibition of androgen synthesis results in a high response rate in castration refractory prostate cancer. 98th Annual Meeting for American Association for Cancer Research; 2007 April 17; Los Angeles, CA. 2007.
10. Njar VC, Brodie AM. Inhibitors of 17α-hydroxylase/17,20-lyase (CYP17): potential agents for the treatment of prostate cancer. Curr Pharm Des. 1999; 5:163–80. [PubMed: 10066888]
11. Handratta VD, Vasaitis TS, Njar VC, et al. Novel C-17-heteroaryl steroidal CYP17 inhibitors/antiandrogens: synthesis, *in vitro* biological activity, pharmacokinetics, and antitumor activity in the LAPC4 human prostate cancer xenograft model. J Med Chem. 2005; 48:2972–84. [PubMed: 15828836]
12. Perkins LM, Payne AH. Quantification of P450scc, P450(17) α, and iron sulfur protein reductase in Leydig cells and adrenals of inbred strains of mice. Endocrinology. 1988; 123:2675–82. [PubMed: 2848682]
13. Kaufman RJ. Stress signaling from the lumen of the endoplasmic reticulum: coordination of gene transcriptional and translational controls. Genes Dev. 1999; 13:1211–33. [PubMed: 10346810]
14. Mori K. Tripartite management of unfolded proteins in the endoplasmic reticulum. Cell. 2000; 101:451–4. [PubMed: 10850487]
15. Liu H, Bowes RC III, van de Water B, Sillence C, Nagelkerke JF, Stevens JL. Endoplasmic reticulum chaperones GRP78 and calreticulin prevent oxidative stress, Ca2+ disturbances, and cell death in renal epithelial cells. J Biol Chem. 1997; 272:21751–9. [PubMed: 9268304]
16. Harding HP, Zhang Y, Ron D. Protein translation and folding are coupled by an endoplasmic-reticulum-resident kinase. Nature. 1999; 397:271–4. [PubMed: 9930704]
17. Shi Y, Vattem KM, Sood R, et al. Identification and characterization of pancreatic eukaryotic initiation factor 2 α-subunit kinase, PEK, involved in translational control. Mol Cell Biol. 1998; 18:7499–509. [PubMed: 9819435]
18. Clemens MJ. Targets and mechanisms for the regulation of translation in malignant transformation. Oncogene. 2004; 23:3180–8. [PubMed: 15094767]
19. Aktas H, Fluckiger R, Acosta JA, Savage JM, Palakurthi SS, Halperin JA. Depletion of intracellular Ca2+ stores, phosphorylation of eIF2α, and sustained inhibition of translation initiation mediate the anticancer effects of clotrimazole. Proc Natl Acad Sci U S A. 1998; 95:8280–5. [PubMed: 9653178]
20. Lai E, Teodoro T, Volchuk A. Endoplasmic reticulum stress: signaling the unfolded protein response. Physiology. 2007; 22:193–201. [PubMed: 17557940]
21. Prostko CR, Brostrom MA, Brostrom CO. Reversible phosphorylation of eukaryotic initiation factor 2α in response to endoplasmic reticular signaling. Mol Cell Biochem. 1993; 127–128:255–65.
22. Ron D. Translational control in the endoplasmic reticulum stress response. J Clin Invest. 2002; 110:1383–8. [PubMed: 12438433]
23. Zinszner H, Kuroda M, Wang X, et al. CHOP is implicated in programmed cell death in response to impaired function of the endoplasmic reticulum. Genes Dev. 1998; 12:982–95. [PubMed: 9531536]
24. Palakurthi SS, Fluckiger R, Aktas H, et al. Inhibition of translation initiation mediates the anticancer effect of the n-3 polyunsaturated fatty acid eicosapentaenoic acid. Cancer Res. 2000; 60:2919–25. [PubMed: 10850438]
25. Sun S, Han J, Ralph WM Jr, et al. Endoplasmic reticulum stress as a correlate of cytotoxicity in human tumor cells exposed to diindolylmethane *in vitro*. Cell Stress Chaperones. 2004; 9:76–87. [PubMed: 15270080]
26. Little JL, Wheeler FB, Fels DR, Koumenis C, Kridel SJ. Inhibition of fatty acid synthase induces endoplasmic reticulum stress in tumor cells. Cancer Res. 2007; 67:1262–9. [PubMed: 17283163]
27. Pyrko P, Kardosh A, Liu YT, et al. Calcium-activated endoplasmic reticulum stress as a major component of tumor cell death induced by 2,5-dimethyl-celecoxib, a non-coxib analogue of celecoxib. Mol Cancer Ther. 2007; 6:1262–75. [PubMed: 17431104]

28. Njar VC, Kato K, Nnane IP, Grigoryev DN, Long BJ, Brodie AM. Novel 17-azolyl steroids, potent inhibitors of human cytochrome 17 α-hydroxylase-C17,20-lyase (P450(17) α): potential agents for the treatment of prostate cancer. J Med Chem. 1998; 41:902–12. [PubMed: 9526564]
29. Potter GA, Barrie SE, Jarman M, Rowlands MG. Novel steroidal inhibitors of human cytochrome P45017α (17α-hydroxylase-C17,20-lyase): potential agents for the treatment of prostatic cancer. J Med Chem. 1995; 38:2463–71. [PubMed: 7608911]
30. Potter GA, Hardcastle IR, Jarman M. A Convenient, Large-Scale Synthesis of Abiraterone Acetate [β-Acetoxy-17-(3-pyridyl)androsta-5,16-dien], A Potential New Drug for the Treatment of Prostate Cancer. Organic Preperations and Procedures Int. 1997; 29:123–34.
31. Patel JB, Huynh CK, Handratta VD, et al. Novel retinoic acid metabolism blocking agents endowed with multiple biological activities are efficient growth inhibitors of human breast and prostate cancer cells *in vitro* and a human breast tumor xenograft in nude mice. J Med Chem. 2004; 47:6716–29. [PubMed: 15615521]
32. Chou TC, Tan QH, Sirotnak FM. Quantitation of the synergistic interaction of edatrexate and cisplatin *in vitro*. Cancer Chemother Pharmacol. 1993; 31:259–64. [PubMed: 8422687]
33. Khandelwal A, Gediya LK, Njar VC. MS-275 synergistically enhances the growth inhibitory effects of RAMBA VN/66–1 in hormone-insensitive PC-3 prostate cancer cells and tumours. Br J Cancer. 2008; 98:1234–43. [PubMed: 18349838]
34. Grynkiewicz G, Poenie M, Tsien RY. A new generation of Ca2+ indicators with greatly improved fluorescence properties. J Biol Chem. 1985; 260:3440–50. [PubMed: 3838314]
35. Navone NM, Logothetis CJ, von Eschenbach AC, Troncoso P. Model systems of prostate cancer: uses and limitations. Cancer Metastasis Rev. 1998; 17:361–71. [PubMed: 10453280]
36. Lecca MR, Wagner U, Patrignani A, Berger EG, Hennet T. Genome-wide analysis of the unfolded protein response in fibroblasts from congenital disorders of glycosylation type-I patients. FASEB J. 2005; 19:240–2. [PubMed: 15545299]
37. Arumugam T, Simeone DM, Schmidt AM, Logsdon CD. S100P stimulates cell proliferation and survival via receptor for activated glycation end products (RAGE). J Biol Chem. 2004; 279:5059–65. [PubMed: 14617629]
38. Beer DG, Kardia SL, Huang CC, et al. Gene-expression profiles predict survival of patients with lung adenocarcinoma. Nat Med. 2002; 8:816–24. [PubMed: 12118244]
39. Jiang F, Shults K, Flye L, et al. S100P is selectively upregulated in tumor cell lines challenged with DNA cross-linking agents. Leuk Res. 2005; 29:1181–90. [PubMed: 15936073]
40. Shyu RY, Huang SL, Jiang SY. Retinoic acid increases expression of the calcium-binding protein S100P in human gastric cancer cells. J Biomed Sci. 2003; 10:313–9. [PubMed: 12711858]
41. Lukas J, Herzinger T, Hansen K, et al. Cyclin E-induced S phase without activation of the pRb/E2F pathway. Genes Dev. 1997; 11:1479–92. [PubMed: 9192874]
42. Savino JA III, Evans JF, Rabinowitz D, Auborn KJ, Carter TH. Multiple, disparate roles for calcium signaling in apoptosis of human prostate and cervical cancer cells exposed to diindolylmethane. Mol Cancer Ther. 2006; 5:556–63. [PubMed: 16546969]
43. Zhang Y, Soboloff J, Zhu Z, Berger SA. Inhibition of Ca2+ influx is required for mitochondrial reactive oxygen species-induced endoplasmic reticulum Ca2+ depletion and cell death in leukemia cells. Mol Pharmacol. 2006; 70:1424–34. [PubMed: 16849592]
44. O'Donnell A, Judson I, Dowsett M, et al. Hormonal impact of the 17α-hydroxylase/C(17, 20)-lyase inhibitor abiraterone acetate (CB7630) in patients with prostate cancer. Br J Cancer. 2004; 90:2317–25. [PubMed: 15150570]
45. Moenner M, Pluquet O, Bouchecareilh M, Chevet E. Integrated endoplasmic reticulum stress responses in cancer. Cancer Res. 2007; 67:10631–4. [PubMed: 18006802]

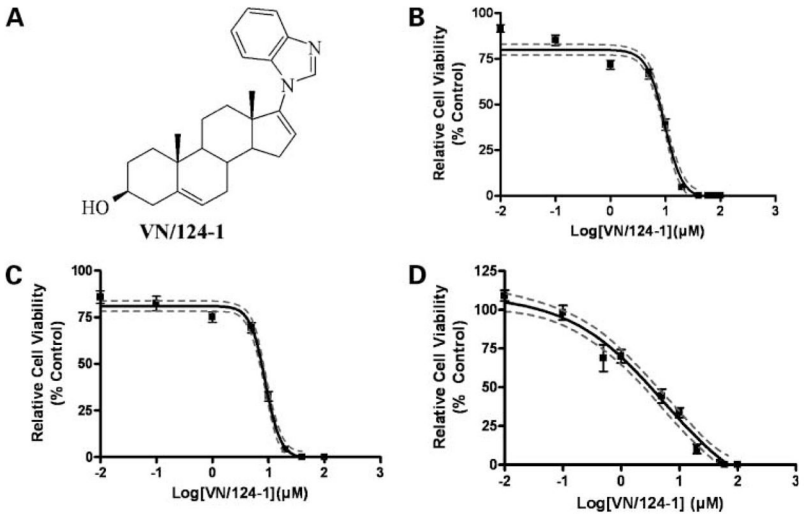

Figure 1.

VN/124-1 inhibits the growth of androgen-insensitive PC-3 and DU-145 cells, as well as androgen-dependent LNCaP cells. **A,** structure of VN/124-1. Cell viability curves for PC-3 (**B**), DU-145 (**C**), and LNCaP (**D**) generated from an MTT assay after 96-h exposure to VN/124-1, as described in Materials and Methods. *Points*, mean of 18 replicates from three independent experiments; *bars*, SE. *Solid line*, best-fit sigmoidal-dose response (variable slope); *dotted lines*, 95% confidence interval.

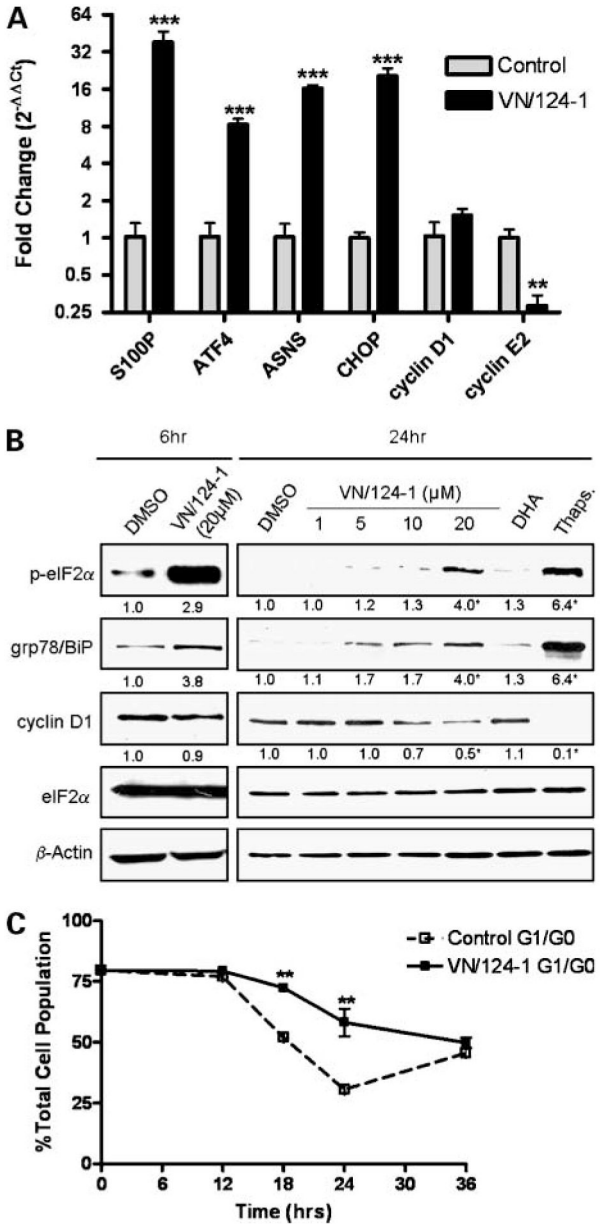

Figure 2.

VN/124-1 induces the ERSR resulting in G_1-G_0 cell cycle arrest. **A,** qRT-PCR assessment of stress response and cell cycle– related genes in PC-3 cells after 24 h exposure to 20 μmol/L VN/124-1. Expression is measured as fold change relative to control. **B,** representative Western blots after 6 and 24 h treatment with VN/124-1, 500 nmol/L of the known ERSR-inducer thapsigargin (*Thaps.*), or 20 μmol/L DHA in PC-3. Numbers under the panels represent the mean fold change relative to control as measured by densitometry. **C,** effect of 20 μmol/L VN/124-1 cell cycle progression. PC-3 cells were synchronized in G_1-G_0 by serum starvation for 96 h. Cells were then incubated with full-growth medium containing either vehicle or 20 μmol/L VN/124-1, and cell cycle was assessed at relative

time points by flow cytometry. *Points*, mean of three independent experiments; *bars*, SE. *, $P < 0.05$; **, $P < 0.01$; ***, $P < 0.001$.

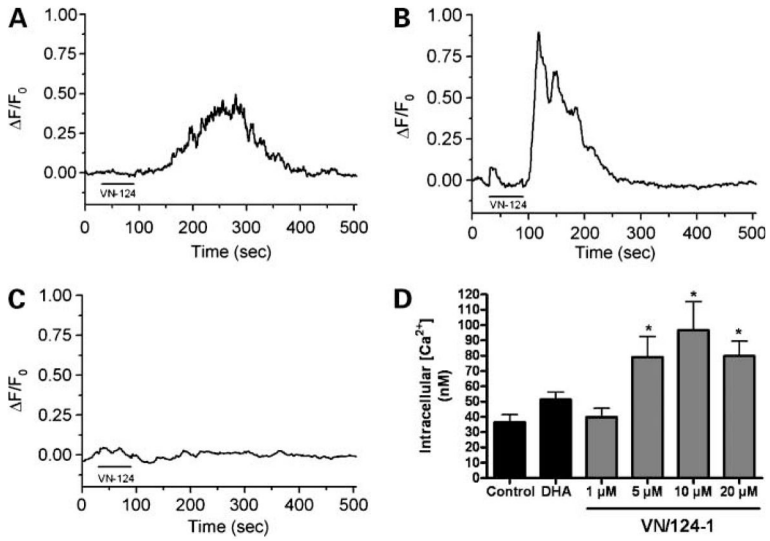

Figure 3.

VN/124-1 induces release of calcium from ER. PC-3 cells loaded with Fluo-3AM were treated with 20 μmol/L VN/124-1 in the presence (**A**) or absence (**B**) of extracellular calcium. Mean peak values are 0.613 and 0.967, respectively. **C,** PC-3 cells were pretreated for 5 min with cyclopiazonic acid before dosing with 20 μmol/L VN/124-1. For all treatments, Ca^{2+} transients were measured in individual cells (n = 9, 12, and 9, respectively), as described in Materials and Methods. **D,** cells were dosed with increasing concentrations of VN/124-1, 20μmol/L DHA, or vehicle for 2 h and then loaded with Fura-2AM and absolute [Ca^{2+}] were measured. Individual cells were counted (n = 32) as described in Materials and Methods. *, $P < 0.05$.

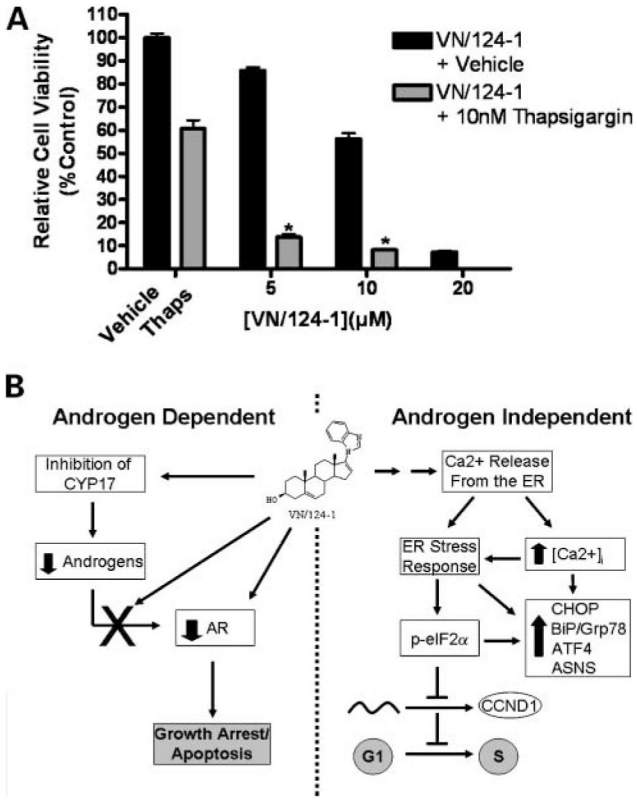

Figure 4.

A, combination of VN/124-1 and thapsigargin. PC-3 cells were treated with 5, 10, or 20 μmol/L VN/124-1 plus 10 nmol/L thapsigargin or vehicle (DMSO) for 96 h, and cell viability was assessed via MTT assay. The combination was synergistic in inhibiting PC-3 cell growth at all three (combination index = 0.40, 0.58, and 0.77, respectively). *, $P < 0.01$. **B,** scheme of androgen-dependent and androgen-independent mechanisms of action of VN/124-1.

Table 1

Growth inhibitory effects of steroidal lyase inhibitors against PC-3, DU-145, and LNCaP cells

Compound	Cell line	GI_{50} (μmol/L)	95% CI (μmol/L)	GI_{90} (μmol/L)	95% CI (μmol/L)
VN/63-1	PC-3	2.91	1.14–11.57	>100	—
VN/85-1		1.86	1.31–2.86	30.41	13.18–67.61
VN/124-1		7.82	7.13–8.38	18.62	16.10–21.88
VN/125-1		1.41	1.22–1.60	8.07	6.61–9.80
Abiraterone		9.32	8.69–9.94	>100	—
VN/63-1	DU-145	11.04	4.75–22.74	>100	—
VN/85-1		5.31	3.71–7.22	31.62	23.12–40.58
VN/124-1		7.55	6.90–8.11	15.95	13.86–18.24
VN/125-1		6.57	5.58–7.51	15.53	12.40–19.55
Abiraterone		14.68	13.42–15.95	>100	—
VN/63-1	LNCaP	1.05	0.69–1.55	>100	—
VN/85-1		2.47	1.55–3.96	36.49	23.03–58.74
VN/124-1		3.15	2.41–4.17	31.99	23.82–45.01
VN/125-1		1.18	0.95–1.48	13.46	9.80–18.01
Abiraterone		1.41	0.95–1.96	25.12	14.19–100

NOTE: Cells were treated with various concentrations of each compound for 96 h, and cell viability was assessed by MTT assay, as described in Materials and Methods. GI_{50} and GI_{90} values were calculated from sigmoidal-dose response curves (variable slope) generated from three independent experiments.

Abbreviation: 95% CI, 95% confidence interval.

Table 2

VN/124-1 up-regulated and down-regulated ontologies

	Count	%	*P*
Up-regulated ontology			
Response to stress	16	24.24	1.93E-05
Amino acid metabolism	8	12.12	6.97E-05
Amine metabolism	9	13.64	1.01E-04
Nitrogen compound metabolism	9	13.64	1.61E-04
Amino acid and derivative metabolism	8	12.12	1.77E-04
Negative regulation of biological process	12	18.18	1.90E-04
Negative regulation of cellular process	11	16.67	4.57E-04
Development	18	27.27	6.29E-04
Carboxylic acid metabolism	9	13.64	7.48E-04
Organic acid metabolism	9	13.64	7.68E-04
Response to external stimulus	9	13.64	9.76E-04
Down-regulated ontology			
DNA replication	17	34.69	3.82E-19
DNA metabolism	19	38.78	2.98E-13
DNA-dependent DNA replication	10	20.41	6.88E-12
Cell cycle	16	32.65	1.41E-09
Biopolymer metabolism	27	55.1	1.51E-08
Regulation of progression through cell cycle	10	20.41	9.25E-06
Regulation of cell cycle	10	20.41	9.41E-06
Nucleobase, nucleoside, nucleotide and nucleic acid metabolism	24	48.98	8.12E-05
Macromolecule metabolism	28	57.14	9.94E-05
Second messenger–mediated signaling	6	12.24	2.86E-04

NOTE: Up-regulated and down-regulated ontologies were identified using Database for Annotation, Visualization, and Integrated Discovery, as described in Materials and Methods for genes up-regulated in PC3 cells by 24-h exposure to 20 μmol/L VN/124-1, as determined by affymetrix human focus microarray. *P* values are based on an enrichment (EASE) score.